

Design of Intelligent Obstacle Avoidance System for Fully Automated Unmanned Vehicle Based on Laser Ranging

Chunyuan Li *

Institute of Mathematics and Statistics, Baicheng Normal University, Baicheng 137000, China

Received OCT 16 2019

Accepted FEB 4 2020

Abstract

The vehicle obstacle avoidance system based on fuzzy neural network uses the fuzzy neural network to extract the road obstacle information, and has not designed the obstacle avoidance path, which has the disadvantage of low correct rate of obstacle avoidance results. An intelligent obstacle avoidance system for fully automated unmanned vehicle based on laser ranging is designed. The system consists of three parts: information acquisition, information processing and information control. The hardware consists of laser rangefinder, controller module, motor module and GPS positioning system. The laser rangefinder obtains obstacle information by using pulsed infrared laser beam and transmits measurement information in real time. The main engine of fully automated unmanned vehicle is given information processing to realize effective obstacle detection. The system adopts obstacle avoidance path and obstacle avoidance process based on grid-ant colony algorithm to realize intelligent obstacle avoidance of fully automated unmanned vehicle. The correct rate of obstacle avoidance to static and dynamic obstacles in the designed system is 100%. The system is an intelligent obstacle avoidance system for fully automated unmanned vehicle with high precision and high application value.

© 2020 Jordan Journal of Mechanical and Industrial Engineering. All rights reserved

Keywords laser ranging; automated; unmanned vehicle; intelligent obstacle avoidance; system design; grid-ant colony.

1. Introduction

Fully automated unmanned vehicle is a kind of intelligent vehicle which does not need to be driven by human, and it can also be regarded as a four-wheeled robot. It consists of three systems: sensor system, main control computer system and automatic driving system. It relies on a variety of precise sensors, laser rangefinders and acoustic radar before and after the vehicle to collect information about the surrounding environment. Then the collected information is transported to the main controller system through processing and transformation, and the main controller issues commands to make the driving system drive safely and correctly, so as to realize unmanned driving [1]. Nowadays, the main problem of fully automated unmanned driving is the simplicity of driving, that is, there are too few kinds of assumptions about the road condition to control the whole road condition like human beings. The unmanned driving on the highway is more mature, because the highway road conditions are relatively easy to achieve automatic control. Secondly, the collection of all kinds of information on the road is not complete, only the specific and simple road information can be used, and the handling of unexpected situations lacks great adaptability.

Obstacle avoidance is a basic function of autonomous mobile robots. Many scholars have done a lot of research on it. The basic idea of potential field method is that the mobile space of robots is a virtual force field [2]. The target point generates gravity, the obstacle generates repulsion, and the robot moves under the resultant force of gravity and repulsion. The information is simplified to a single resultant force, and the details of local obstacles are lost [3-5]. The Vector Field Histogram (VFH) takes the mobile robot as the center to establish a 1-D polar histogram to represent the environment. The linear and angular velocities are controlled separately. The curvature velocity method can better solve the problem of losing the details of the environment by a single resultant force of the potential field method. Curvature-velocity method and dynamic window transform obstacle avoidance problem into the constrained optimization problem of linear-angular velocity space.

Laser range finder is a kind of active imaging laser sensor, which is not affected by the change of illumination. It has short wave length, fast scanning speed and easy installation. It is widely used in automobile anti-collision and line-patrolling robot. In order to accurately acquire the obstacle information of fully automated unmanned vehicle on the moving path, an intelligent obstacle avoidance system of fully automatic unmanned vehicle based on laser

* Corresponding author e-mail: chunyuanyuanli0410@163.com.

ranging is designed by using laser rangefinder to collect obstacle information.

2. Materials and Methods

2.1. Intelligent Obstacle Avoidance System of Fully Automated Unmanned Vehicle based on Laser Ranging

The system consists of three parts: information acquisition, information processing and information control. The acquisition information system ascertains the fixed obstacles from the GIS investigation of the regional environment, and then uses the grid-ant colony algorithm to plan the path and get the obstacle avoidance parameters. It is introduced into the LabVIEW software system and runs the collision avoidance algorithm to complete the obstacle avoidance design of the fixed obstacles. The measurement of random obstacles is to transmit the information measured by laser rangefinder to the data processor of software. During the operation of the information processing system, the automated unmanned vehicle uses the method of automatic staying to judge the movement form of random obstacles and to plan the next forward path so as to enable the information control system to have the functions of autonomous navigation and obstacle avoidance and complete the task of intelligent obstacle avoidance [6]. Finally, it forms the circulation, coherence and integrity of information collection, information processing and information control. The overall design of the system is shown in Figure 1.

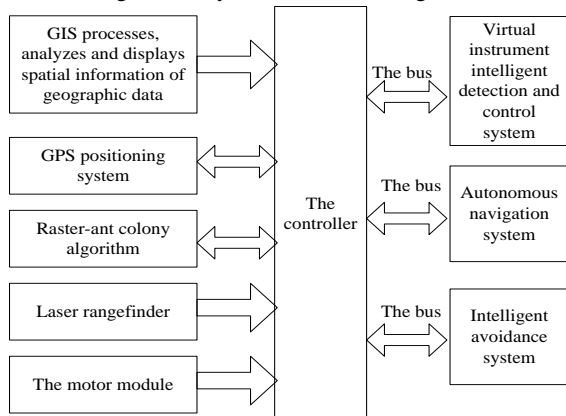


Figure 1. Overall structure of the system.

2.2. System Hardware Design

2.2.1. Laser Range Finder

Laser range finder is a high precision and high resolution external sensor based on TOF (Time of Flight) principle. The laser rangefinder has an operating temperature of -10°C to $+50^{\circ}\text{C}$, a detection frequency of $1/6$ to $1/3\text{HZ}$, and a field of view of 6.5° .

Taking LMS 200 of SICK Company in Germany as an example, its scanning area is 180° , the scanning direction is counterclockwise, the maximum limited distance is 8 m, and the resolution of distance and angle is 15 mm and 1° , respectively. It has the advantages of fast scanning (scanning cycle is 13.3 ms), dense data points and high measurement accuracy. In order to reduce the adverse effects caused by the uneven intensity of reflected light, LMS200 uses the binary method to deal with the intensity

of reflected light [7], which is insensitive to environmental light, mainly affected by obstacle materials and surface smoothness.

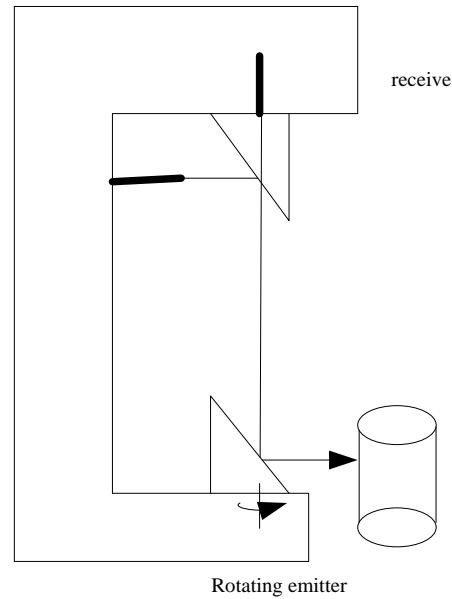


Figure 2. of laser rangefinder.

LMS200 laser range finder is a non-contact active ranging system, which does not need preset transmitter and location mark. Its working principle is based on the measurement of laser beam's flight time, as shown in Figure 2. Pulsed infrared laser beams are emitted and reflected back when they encounter objects, and recorded by the receiver of the range finder. The time of laser pulse transmitting and receiving is proportional to the distance between the distance meter and the measured object. The pulsed laser beam is deflected by a rotating light mirror (rotating speed is 75 rps) inside the range finder to form a sector scanning area for the surrounding environment. The contour of the target object is determined from a series of pulses received. Through high-speed serial interface (500 kbit/s RS422), real-time measurement data can be transmitted to the main engine of fully automated unmanned vehicle for further data processing [8-11]. The scanning data coordinates of the laser rangefinder are shown as follows:

$$G_n = (d_n, \phi_n)^T, n = 1, \dots, N \quad (1)$$

Where, d_n represents the amount of data transmission, ϕ_n represents the measurement angle of an object, T represents measurement time.

Cartesian coordinate can be expressed as:

$$H_n = (x_n, y_n)^T, n = 1, \dots, N \quad (2)$$

Where $x_n = d_n \cos \phi_n$, $y_n = d_n \sin \phi_n$, N is the number of scanned data.

2.2.2. Controller Module Design

The hardware of the intelligent obstacle avoidance system of fully automated unmanned vehicle based on laser ranging mainly adopts the controller to realize the obstacle avoidance of the vehicle. The controller mainly includes two parts: the host computer and the slave computer. The host computer and the slave computer exchange data mainly through RS232 serial communication cable, and realize the embedded connection. The controller structure is shown in Figure 3.

The host computer refers to the module that controls the mobile robot directly [12-14], including the data collection module, the direct control module and the touch screen display module of the laser range finder. The slave computer refers to the indirect control module of the laser range finder, including the camera, the embedded control chip and the motor drive circuit. The slave computer is mainly responsible for collecting the signal of the laser range finder and the external environment information [15-18], and make the control plan according to the intelligent control algorithm. The host computer is responsible for displaying the data in the slave computer and making management through analysis and judgment. It can also directly issue control commands to the slave computer.

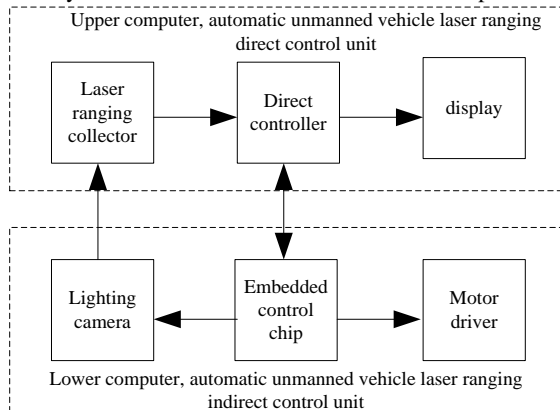


Figure 3. Structure diagram of the controller.

2.2.2. Motor Module Design

The obstacle avoidance system of fully automated unmanned vehicle adopts DC motor drive mode, which controls the forward, backward or left-right steering of the vehicle by controlling left and right DC current. As shown in figure 4, DC motor adopts DC motor driver chip L298N, and double-bridge motor driver chip L298 has maximum output current of 4 amperes, which has over-temperature protection function and high noise suppression ratio. The output just meets the driving requirements of the left and right DC motor of the vehicle. The operation state of the motor can be controlled by the level input of three L298N input ports. The working state of the motor is shown in Table 1.

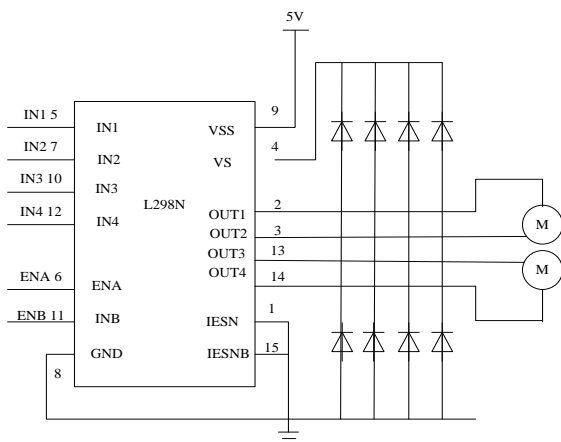


Figure 4. Motor module.

Table 1. DC motor operating status.

ENA	IN1	IN2	Running condition
0	X	X	Stop
1	1	0	Forward
1	0	1	Reverse
1	1	1	Brake
1	0	0	Stop

2.3. System Implementation

2.3.1. Obstacle Avoidance Path based on Grid-Ant Colony Algorithm

The system adopts the principle of avoiding collision based on grid-ant colony algorithm. The grid method is a kind of approximate discrete data which is approximated by a finite grid. Its row array is easy to store, operate, display and maintain for computer. The size of the grid determines the accuracy of the geographic data in the coverage area, and they are inversely proportional, so the finer the grid element is, the more accurate the grid data is. The grid method is the preferred method for system path planning: firstly, the space of a known region is made into a grid network model, including the location and size of the fixed obstacles in the region [19]; secondly, the size of the grid is determined by the accuracy of the path. Because the vehicle and obstacle cannot be in the same grid when avoiding obstacles, the safe distance between the vehicle and obstacle is at least twice the grid edge length. Finally, the grid of the region and the fixed obstacle is coded. Ant colony algorithm (ACA) is a probabilistic algorithm used to find the optimal path in the graph. Ant colony algorithm has been successfully applied in several fields. The proposed algorithm is applied to vehicle intelligent obstacle avoidance system to ensure the accuracy of autonomous obstacle avoidance [20]. The system adopts the principle of avoidance based on raster-ant colony algorithm, and does not take constant as the initial pheromone, so as to reduce the number of times that ants fail to find the path, and to ensure the accuracy of intelligent obstacle avoidance. The whole process is shown in Figure 5: white grid represents feasible grid, black grid represents infeasible grid, starting point is S , target point is O .

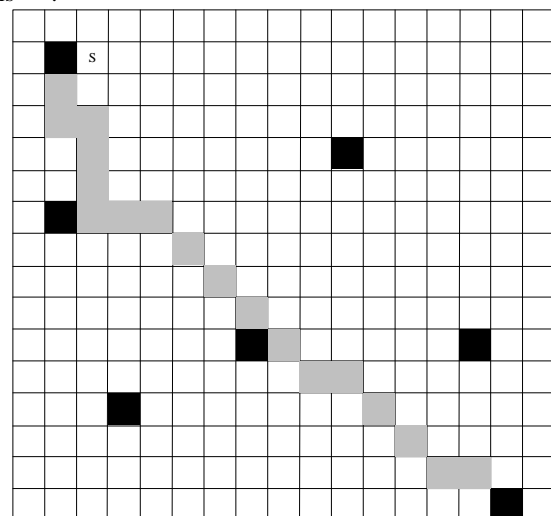


Figure 5. Grid - ant algorithm design drawing.

Assuming that there are K ants searching for the target O from the starting point S , the ant can only walk one step to the adjacent non-obstacle grid around it. Assuming that the k -th ant is in the first square, the probability that it chooses the next square j is:

$$P_{ij}^k = \frac{(\tau_j)^\alpha (\eta_{ij})^\beta}{\sum_j (\tau_j)^\alpha (\eta_{ij})^\beta} \quad (3)$$

Where: τ_j denotes the content of pheromones in the grid j ; $\eta_{ij} = 1/d_{ij}$ denotes the reciprocal of the distance between the grid i and j ; α and β are constants, usually $1 \leq \alpha \leq 2.2 \leq \beta \leq 5$. Each ant sprays a certain pheromone in the square it passes after it has completed its journey.

$$\Delta\tau_k = Q/L_k \quad (4)$$

Where L_k denotes the length of the path taken by the k -th ant; Q is a constant. If an ant fails to find the target O , it searches again until it finds a feasible route [21-23]. After all the ants have found the target O , the pheromones in each square is updated with the following formula:

$$\tau_{n+1} = \rho\tau_n + \sum_{k=1}^K \Delta\tau_k \quad (5)$$

Where ρ is the degree of retention of pheromones.

The path planning of system obstacle avoidance design is as follows:

Step 1: Let the planned path be a directed polygon with X points.

Step 2: Run along the original planning path.

Step 3: Automated unmanned vehicles will have random obstacles when they drive on the set route independently.

Step 4: When a random obstacle is measured by a laser rangefinder, the coordinates of the current vehicle are obtained, and the size of D and L is compared (where D is the distance between the vehicle and the obstacle and L is the distance between the vehicle and the next sub-target).

Step 5: in first comparison, if $D > L$, it thinks there is no obstacle, continue to move forward, laser detector has been used to measure. Return the comparison of D and L to step 4.

Step 6: in the initial comparison, if $D < L$, it proves that there is an obstacle. At this time, the vehicle will wait for the set time t in situ. When there is no obstacle at time t , it will follow the original path.

Step 7: When there is an obstacle in Time t measurement, the vehicle stays and regards the random obstacle as a fixed obstacle to use the system to re-plan the path; or when the volume of the obstacle is relatively small, the vehicle steers to the feasible grid adjacent to the obstacle to avoid the obstacle. In order to achieve the optimal path planning for obstacle avoidance, the system compares the results of partial re-planning with the results of back-to-the-original path movement after corner, and chooses the best path.

Step 8: If it encounters another obstacle, go back to step 4 and recycle. If there is no random obstacle, run directly to the final target point.

2.3.2. Implementation Process of Obstacle Avoidance

The system controller is based on ARM (Advanced RISC Machines) embedded platform and S3C2440 microprocessor chip. It supports SD card slot and 256M memory configuration. The interface is relatively rich. It can transmit and store pictures, videos and multi-dimensional data. It can reasonably reduce the control delay. Receiving the teaching information of the instructor, kinematics calculation and trajectory planning are carried out based on it, and communication is realized by RS485 bus to ensure the coordinated movement of all links [24]. The microprocessor chip S3C2440 controls the direct controller with the host computer and the camera and servo driver of the slave computer. The chip is the core of the whole control system. It can accurately control the driving frequency and pulse number of the motor and directly decode, encode and compress the data in the controller. The embedded technology greatly simplifies the design cost and the complexity of implementation [25-27]. As shown in Figure 6, the intelligent obstacle avoidance process of fully automated unmanned vehicle is controlled by laser rangefinder.

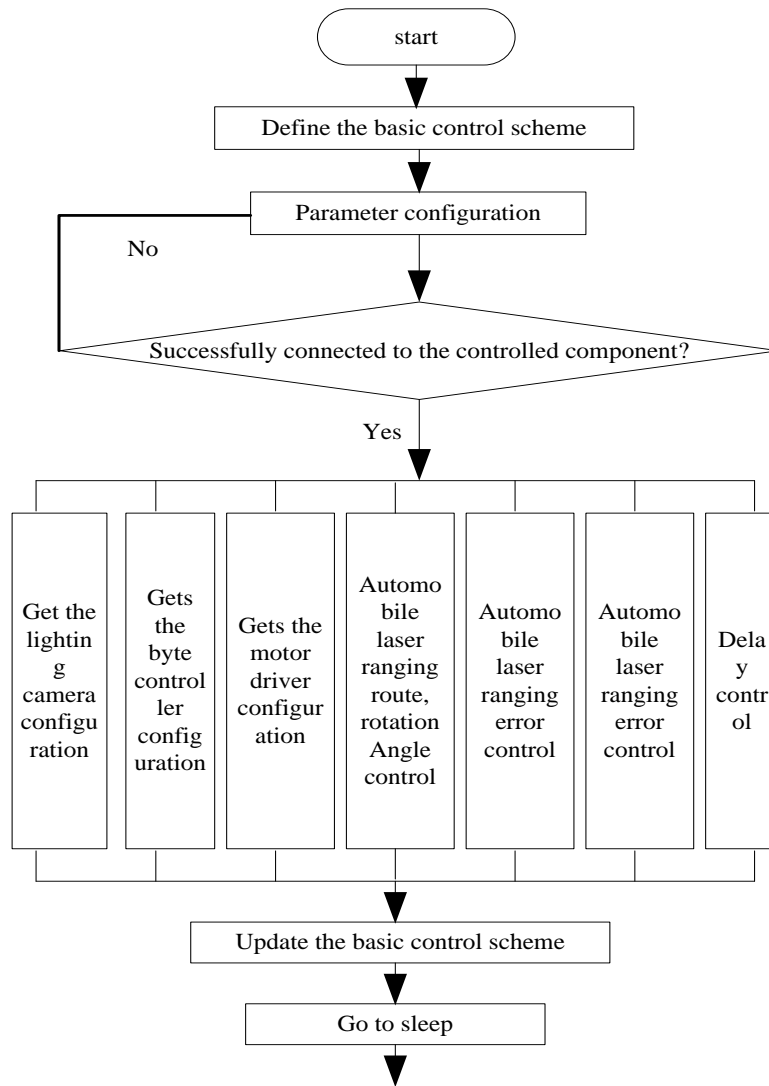


Figure 6. Obstacle avoidance control flow of fully automatic unmanned vehicle with laser rangefinder.

3. 3. Results

3.1. Analysis of Obstacle Avoidance Effect

In order to verify the feasibility and effectiveness of the designed system, the unmanned vehicle shown in Figure 7 is simulated in the obstacle avoidance test chart of Figure 8. Static obstacle avoidance test and dynamic obstacle avoidance test are carried out respectively. Figure 9 shows that the obstacle avoidance system designed in this paper can completely avoid static obstacles and effectively avoid collision with static obstacles during vehicle movement.

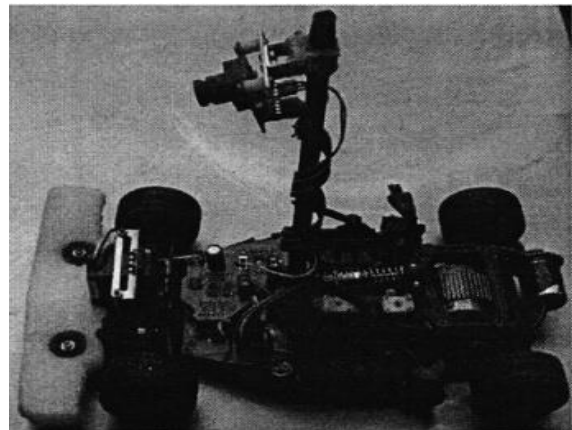


Figure 7. Physical drawing of fully automatic unmanned car.

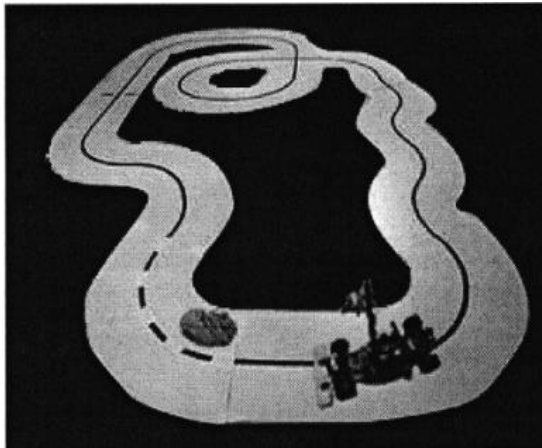


Figure 8. Obstacle avoidance test route.

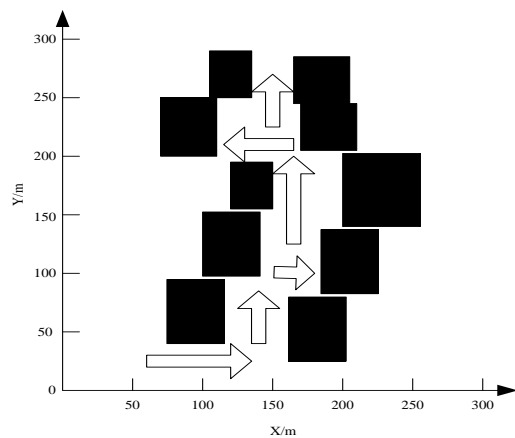


Figure 9. The movement track of the intelligent obstacle avoidance static obstacle driven by an automatic uav.

In the course of driving a fully automated UAV (Unmanned Aerial Vehicle), the obstacles in the path of motion are always in the state of motion, that is, they have dynamic characteristics. Therefore, the robot must have self-adaptability and adjustability when moving. Figure 10 is the path of the robot in the environment with dynamic obstacles. As can be seen from Figure 10, the system designed in this paper is also applicable to obstacle avoidance. The vehicle can adjust its motion path adaptively to avoid path obstacles effectively, which proves that the system in this paper has strong flexibility and adaptability.

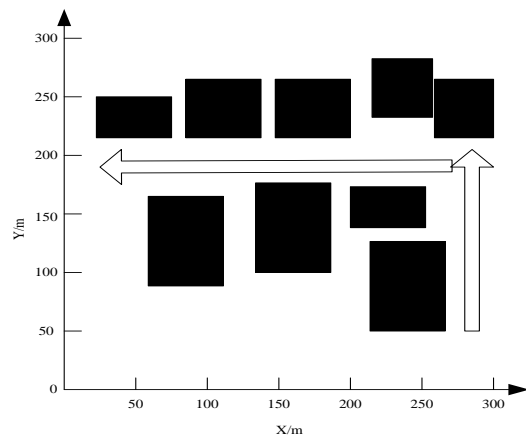


Figure 10. Trajectory of intelligent obstacle avoidance and dynamic obstacle avoidance in a fully automatic uav driving vehicle.

3.2. Correct Analysis of Obstacle Avoidance Results

On the basis of the above experimental results, the experiment further verifies the accuracy of the intelligent obstacle avoidance results of this system. In order to highlight the high accuracy of obstacle avoidance in practical application of the designed system, 14 static obstacles with different distances are set up in the laboratory, and the obstacle avoidance results of the vehicle obstacle avoidance system based on fuzzy neural network and visual positioning are taken as experimental reference. The accuracy of obstacle avoidance of the three systems at different distances from obstacles is compared and analyzed. The experimental results of the three systems are described in Tables 2, 3 and 4, respectively.

Table 2. The static obstacle avoidance results of the proposed system.

The standard distance/cm	Car travel distance /cm	Distance from obstacles /cm	Successful obstacle avoidance
20	19.8	0.2	Yes
40	36.5	3.5	yes
60	58.6	1.4	yes
80	76.5	3.5	yes
100	98.6	1.4	yes
150	147.5	2.5	yes
200	195.6	4.4	yes
250	245.6	4.4	yes
300	282.6	7.4	yes
400	396.4	3.6	yes
500	418.9	1.1	yes
600	596.2	3.8	yes
700	616.5	3.5	yes
800	795.4	4.6	yes

The results of Table 2 show that the system has a good effect on avoiding static obstacles. Detailed analysis of the data in the table shows that all fully automated unmanned vehicles can stop at a certain distance from the obstacles in the test and avoid collision with the obstacles. From the third column of the table, it can be concluded that when the system detects obstacles in a certain position in front of the vehicle, at the same time, the system can give instructions to the vehicle according to the distance of the obstacle, effectively avoiding the collision between the vehicle and the obstacle. It shows that the system has a good application in intelligent avoidance of collision between fully automatic unmanned vehicle and obstacles.

Table 3. Static obstacle avoidance based on fuzzy neural network and obstacle avoidance system.

The standard distance/cm	Car travel distance /cm	Distance from obstacles /cm	Successful obstacle avoidance
20	26.5	-6.5	no
40	48.6	-8.6	no
60	75.6	-15.6	no
80	66.2	13.8	yes
100	105.5	-5.5	no
150	174.2	-24.2	no
200	224.3	-24.3	no
250	162.4	87.6	yes
300	312.5	-12.5	no
400	416.2	-16.2	no
500	472.3	27.7	yes
600	623.1	-23.1	no
700	706.3	-6.3	no
800	817.4	-17.4	no

The result of data analysis in Table 3 shows that when using the vehicle obstacle avoidance system based on Fuzzy Neural Network to avoid static obstacles, there are

11 experimental tests in which fully automated unmanned vehicles cannot brake within a safe distance, but collide with obstacles, and a certain distance of movement will occur after the collision, which shows that the system is ineffective in avoiding static obstacles and prone to collision accident.

Table 4. Based on the results of visual positioning and static obstacle avoidance system.

The standard distance/cm	Car travel distance /cm	Distance from obstacles /cm	Successful obstacle avoidance
20	23.5	-3.5	no
40	38.6	1.4	yes
60	57.5	2.5	yes
80	75.1	4.9	yes
100	123.1	-23.1	no
150	146.2	3.8	yes
200	223.2	-23.2	no
250	246.5	3.5	yes
300	326.1	-26.1	no
400	367.5	32.5	yes
500	485.2	14.8	yes
600	574.2	25.8	yes
700	736.2	-36.2	no
800	826.7	-26.7	no

From the experimental results in Table 4, it can be seen that the vehicle obstacle avoidance system based on visual positioning has failed six times in many tests, and the number of failures is lower than that of the vehicle obstacle avoidance system based on fuzzy neural network, and lower than that of the system in this paper.

According to the same test method, the correct rate of avoiding dynamic obstacles in three systems is tested. Limited by the limitation of the length of the article, the experiment will arrange 15 different dynamic obstacles in one road plane, and describe the results of avoiding obstacles in three systems with Table 5.

Table 5. Dynamic obstacle avoidance results of the three systems.

Dynamic Obstacle Number	System in this paper	Obstacle Avoidance System based on Fuzzy Neural Network	Obstacle Avoidance System based on Visual Positioning
1	yes	No	no
2	yes	No	yes
3	yes	Yes	no
4	yes	No	no
5	yes	Yes	yes
6	yes	Yes	no
7	yes	No	no
8	yes	Yes	yes
9	yes	No	no
10	yes	Yes	no
11	yes	No	no
12	yes	Yes	no
13	yes	No	yes
14	yes	No	no
15	yes	Yes	yes
Deviation/cm	0.1	2.3	1.2

The results of Table 5 show that the proposed system has a good effect on obstacle avoidance of dynamic obstacles. In the experiment, the system can effectively avoid obstacles every time, and 100% of obstacle avoidance is successful. The deviation value of the proposed system is the smallest, which indicates that the higher the measurement accuracy of the proposed system is. In the experimental test, the success times of the vehicle obstacle avoidance system based on fuzzy neural network and the vehicle obstacle avoidance system based on visual positioning are 7 and 5 times, respectively. The correct rate

of obstacle avoidance is 47% and 33%, respectively. The correct rate of obstacle avoidance for dynamic obstacles is low.

The comprehensive implementation results show that the proposed system has a higher correct rate of obstacle avoidance results for static and dynamic obstacles, and has a better application value in practical applications.

4. Discussion

In this paper, the intelligent obstacle avoidance system of fully automated unmanned vehicle based on laser ranging is designed effectively, but the obstacle avoidance system of fully automated unmanned vehicle is a complex system with human and environment. It is still in the exploratory stage. The future large-scale and wide application of obstacle avoidance system needs further research.

(1) In local obstacle avoidance path planning, virtual obstacles are constructed in straight line segments. In practical applications, fully automated unmanned vehicles often face environments with curved sections or even unstructured roads, which needs to carry out more adaptable obstacle avoidance path planning. This problem can be solved by increasing the number of laser rangefinders or installing panoramic radar.

(2) There is a coupling relationship between longitudinal and lateral motion of fully automated unmanned vehicle. In this paper, the lateral control of the target path tracking control is carried out under the condition of keeping the longitudinal speed stable. By controlling the vehicle chassis to achieve the comprehensive control of the vehicle movement direction, the performance of the automated unmanned vehicle's path tracking control will be further improved.

(3) Because the obstacle avoidance system has good expansibility in both hardware and software resources, it can effectively unify the algorithms of target path tracking control, road and obstacle detection, and apply the results of vehicle condition monitoring to lane maintenance system, adaptive cruise control and vehicle anti-collision system, so as to develop practical vehicle-assisted driving products.

5. Conclusions

In this paper, an intelligent obstacle avoidance system of fully automated unmanned vehicle based on laser ranging is designed. The obstacle information is acquired by laser ranging instrument. The reason why the intelligent obstacle avoidance system of fully automated unmanned vehicle can be accomplished with high quality is as follows:

(1) Laser rangefinder is not affected by the change of illumination. Its wavelength is short, scanning speed is fast, and installation is convenient. It is widely used in automobile collision avoidance and line-patrolling robot.

(2) Using grid-ant colony algorithm for obstacle avoidance path planning can solve the drawbacks of slow speed and easy to fall into local optimum in the process of ant colony algorithm construction. Aiming at the problem that ant colony algorithm is easy to fall into deadlock in the face of concave obstacles, a generalized pheromone updating rule is proposed, which can effectively avoid concave obstacles for fully automated UAV.

Reference

- [1] Guo, J.; Hu, P.; Wang, R. Nonlinear Coordinated Steering and Braking Control of Vision-Based Autonomous Vehicles in Emergency Obstacle Avoidance. *IEEE Transactions on Intelligent Transportation Systems* 2016, 17(11):3230-3240.
- [2] Liu, J.; Jayakumar, P.; Stein, J. L. Combined Speed and Steering Control in High-Speed Autonomous Ground Vehicles for Obstacle Avoidance Using Model Predictive Control. *IEEE Transactions on Vehicular Technology* 2017, 66(10):8746-8763.
- [3] Rosolia, U.; Bruyne, S. D.; Alleyne, A. G. Autonomous Vehicle Control: A Nonconvex Approach for Obstacle Avoidance. *IEEE Transactions on Control Systems Technology* 2017, 25(2):469-484.
- [4] Schaub, A.; Baumgartner, D.; Burschka, D. Reactive Obstacle Avoidance for Highly Maneuverable Vehicles Based on a Two-Stage Optical Flow Clustering. *IEEE Transactions on Intelligent Transportation Systems* 2017, 18(8):2137-2152.
- [5] Graf, P. M.; Bernardini, D.; Esen, H. Spatial-based predictive control and geometric corridor planning for adaptive cruise control coupled with obstacle avoidance. *IEEE Transactions on Control Systems Technology* 2017, (99):1-13.
- [6] Beckmann, H.; Hering, L.; Henze, M. J. Spectral sensitivity in *Onychophora* (velvet worms) revealed by electroretinograms, phototactic behaviour and opsin gene expression. *Journal of Experimental Biology* 2015, 218(Pt 6):915-922.
- [7] Braginsky, B.; Guterma, H. Obstacle Avoidance Approaches for Autonomous Underwater Vehicle: Simulation and Experimental Results. *IEEE Journal of Oceanic Engineering* 2016, 41(4):882-892.
- [8] Erlien, S. M.; Fujita, S.; Gerdes, J. C. Shared Steering Control Using Safe Envelopes for Obstacle Avoidance and Vehicle Stability. *IEEE Transactions on Intelligent Transportation Systems* 2016, 17(2):441-451.
- [9] Shah, B. C.; Švec, P.; Bertaska, I. R. Resolution-adaptive risk-aware trajectory planning for surface vehicles operating in congested civilian traffic. *Autonomous Robots* 2016, 40(7):1139-1163.
- [10] Ali, F.; Kim, E. K.; Kim, Y. G. Type-2 fuzzy ontology-based semantic knowledge for collision avoidance of autonomous underwater vehicles. *Information Sciences* 2015, 295(C):441-464.
- [11] Tang, P.; Zhang, R.; Liu, D. Local reactive obstacle avoidance approach for high-speed unmanned surface vehicle. *Ocean Engineering* 2015, 106:128-140.
- [12] Persiani, F.; Crescenzo, F. D.; Miranda, G. Three-Dimensional Obstacle Avoidance Strategies for Uninhabited Aerial Systems Mission Planning and Replanning. *Journal of Aircraft* 2015, 46(3):832-846.
- [13] Zhang, X.; Zhang, X.; Wang, Y. Extended social force model-based mean shift for pedestrian tracking under obstacle avoidance. *Iet Computer Vision* 2017, 11(1):1-9.
- [14] Guerra, M.; Efimov, D.; Zheng, G. Finite-time obstacle avoidance for unicycle-like robot subject to additive input disturbances. *Autonomous Robots* 2017, 41(1):1-12.
- [15] Vierung, D. H. H. M.; Baaij, J. H. F. D.; Walsh, S. B. Genetic causes of hypomagnesemia, a clinical overview. *Pediatric Nephrology* 2017, 32(7):1123-1135.
- [16] Reynard, F.; Terrier, P. Role of visual input in the control of dynamic balance: variability and instability of gait in treadmill walking while blindfolded. *Experimental Brain Research* 2015, 233(4):1031-1040.
- [17] Mariëlle, W.; Van, O.; Heeren, A.; Smulders, K. Improved gait adjustments after gait adaptability training are associated with reduced attentional demands in persons with stroke. *Experimental Brain Research* 2015, 233(3):1007-1018.
- [18] Ghosh, S.; Panigrahi, P. K.; Parhi, D. R. Analysis of FPA and BA meta-heuristic controllers for optimal path planning of mobile robot in cluttered environment. *Iet Science Measurement & Technology* 2017, 11(7):817-828.
- [19] Lee, B. H.; Jeon, J. D.; Oh, J. H. Velocity obstacle based local collision avoidance for a holonomic elliptic robot. *Autonomous Robots* 2016, 41(6):1-17.
- [20] Maclellan, M. J.; Richards, C. L.; Fung, J. Comparison of kinetic strategies for avoidance of an obstacle with either the paretic or non-paretic as leading limb in persons post stroke. *Gait & Posture* 2015, 42(3):329-334.
- [21] Rauh, N.; Franke, T.; Krems, J. F. Understanding the Impact of Electric Vehicle Driving Experience on Range Anxiety. *Human Factors* 2015, 57(1):177-187.
- [22] Rodrigues, J. A.; Lussi, A.; Seemann, R. Prevention of crown and root caries in adults. *Periodontology* 2015, 55(1):231-249.
- [23] Braña, F. Morphological correlates of burst speed and field movement patterns: the behavioural adjustment of locomotion in wall lizards (*Podarcismuralis*). *Biological Journal of the Linnean Society* 2015, 80(1):135-146.
- [24] Jung, J.; Shin, K.; Sael, L. Random Walk with Restart on Large Graphs Using Block Elimination. *Acm Transactions on Database Systems* 2016, 41(2):1-43.
- [25] Chakraborty A.; Bairagya S.; Sarkar A. Analytical model of surface potential of double surrounding gate mosfet. *Advances in Industrial Engineering and Management*, 2016, 5(1):93-97.
- [26] Yin, L. F.; Yang, B. J.; Wang, C. S. A Multi-Agent Algorithm of Obstacle Avoidance Based on Vectorial Artificial Potential Field. *Computer Simulation* 2016, 41(2):1-43.
- [27] Meng X. B.; Sun S. R. A product conceptual design process model integrating semantics and its support system. *Journal of Mechanical Engineering Research and Developments*, 2016, 39(3):772-781.